

PRODUCTION TECHNOLOGY OF EARLY-HELLENISTIC LIME-BASED MORTARS ORIGINATING FROM A PUNIC-ROMAN RESIDENTIAL AREA IN PALERMO (SICILY)

Giuseppe MONTANA^{1*}, Luciana RANDAZZO¹, Maria Rita CERNIGLIA¹,
Carla ALEO NERO², Francesca SPATAFORA³

¹Dipartimento di Scienze della Terra e del Mare (DiSTeM), University of Palermo, Via Archirafi 36, Palermo, (Italy)

²Soprintendenza Beni Culturali e Ambientali di Palermo, Italy

³Museo Archeologico Antonino Salinas, Palermo, Italy

Abstract

The topic of this study is the mineralogical and petrographic characterization of lime-based mortars of Hellenistic-Roman age (3rd century BCE), collected from a residential area located in the present historical centre of Palermo, near the remains of the Punic-Roman walls. The collected mortars have been analyzed by optical microscopy, X-ray powder diffraction analysis and scanning electron microscopy, coupled with energy-dispersive spectrometry. The aim of the study was the characterization of the mortars as pertaining to their aggregate and binder composition, aggregate size distribution and aggregate/binder ratio, so as to establish the provenance of raw materials and acquire information useful in terms of formulating suitable restoration mortars. The mineralogical and petrographic investigations allowed to recognize four different recipes used for the formulation of the studied mortars. The aggregate is made up of different proportions of alluvial calcareous and siliceous sands or, in some cases, by 'cocciopesto' - opus signinum. Aerial lime-based mortars have been attested for the majority of the wall coatings and decorations subject to analysis. Furthermore, an unusual mosaic flooring, manufactured with tesserae obtained from overfired, locally produced limestone scraps, was attested. The sandy aggregate was quarried from the coastal alluvial deposits of the river Oreto, whose estuary is situated in the vicinity of the ancient city walls. The binder was primarily produced by the calcination of locally available limestones, lacking in magnesium carbonate. It presents a satisfactory technological similarity with two roughly coeval manufactures, located in western Sicily and relating to the aggregate, as well as the mortars manufactured for the purpose of decorating the historical palaces of Palermo. This in turn indicates a remarkable continuity regarding the selection of locally available raw materials, an aspect mainly dictated by their qualitative characteristics.

Keywords: Lime-based mortars; Roman-Hellenistic period; Mineralogical and petrographic characterization; Sicily, Palermo.

Introduction

Mortars are complex composite building materials employed since Classical Antiquity. They consist of a mixture of organic and inorganic binders, aggregates, water and a variety of additives. The relative proportions of the various components should offer suitable workability and appropriate physical, mechanical and aesthetic characteristics to the finished product [1].

* Corresponding author: giuseppe.montana@unipa.it

In recent times, a significant number of studies have focused their attention on the characterization of historical mortars as a source material for important information, especially in the fields of archaeology and conservation [2-6]. The combination of mineralogical, petrographic and chemical investigations with archaeological and historical studies provides data useful for assessing the provenance of raw materials, ancient production technologies and different building phases. On this basis, suitable restoration materials compatible with the original ones can be designed for their respective purposes [7].

In the present work, mineralogical and petrographic investigations were carried out on a set of lime-based mortars dating back to the 4th-3rd century BCE, recovered from a Punic-Roman residential area in Palermo, Sicily. The characterisation of the sampled mortars was carried out by means of the combined use of polarized light microscopy (PLM), X-ray powder diffraction (XRPD) and scanning electron microscopy, coupled with energy-dispersive spectrometry (SEM- EDS). The aim of such research was to determine the compositional and textural characteristics of the sampled mortars, the source of raw materials and the utilized production techniques. It is worth noting that Punic-Roman mortars in Palermo have been never studied from this perspective. On the contrary, several characterization studies were previously carried out on historical mortars and plasters from buildings located in the historical centre of Palermo, mostly manufactured between the 17th century and the 1920's [8-14]. Therefore, an additional research objective was the verification of the continuity of local 'material culture', by comparing compositional and textural features of mortars produced in different historical periods and the criteria followed for the selection of raw materials.

Historical context and archaeological evidences

The city of Palermo, located in Western Sicily, known to the ancients by the name of Panormos, was founded in the 7th century BC by the Phoenicians. The ancient city lay on an emerging Pleistocene calcarenite platform, bordered on its northern extremity by the Tyrrhenian sea, at its southernmost point by a chain of carbonate rock reliefs, approximately 1,000 metres in height (limestones and dolomites of Mesozoic age) and on both sides by two small watercourses (the Oreto and Kemonia rivers). These geomorphological features encouraged the first group of inhabitants to settle in the upmost calcarenite platform (situated approximately 40 metres above sea level), where territorial control was better ensured [15, 16]. The first historical evidence concerning the effective extension of the city, however, dates back to the 3rd century BC, at the time of the Roman conquest. In fact, the ancient historians Polybius and Diodorus described the city as being divided into two different parts, separated from each other by thick walls: the older core was called 'Paleopolis', whereas the relatively more recent city quarters were named 'Neapolis' (Fig. 1A).

The place whence the mortar subject to analysis within the present paper was collected is located in the heart of ancient Palermo, in the area of the Monastero del Gran Cancelliere (also known by the name of Santa Maria de Latinis), founded in 1171 by Matteo Ajello, Chancellor of the Kingdom under William II, King of Normandy at the time. According to the reconstruction realized by archaeologists during the preliminary excavation work carried out in the 1950's in the respective area, different wall structures have been discovered and interpreted as part of the ancient fortification system. A few years previously, after the restoration works that involved the monumental complex of the Monastero del Gran Cancelliere, a huge portion of a defence wall, composed of large local biocalcarene blocks, was brought to light (Fig. 1B and 1C). The wall in question appears to have been part of the network of ancient walls surrounding the Phoenician town on its northern side [17]. Adjacent to a portion of the defense wall, a residential environment, characterized by a peristyle with columns and some remnants of renderings and floorings, was also discovered (Fig. 2A). The archaeological stratigraphical study allowed for its being dated to the middle of the 3rd century BCE. This residential

environment appears to have been abandoned, once it became necessary to reinforce the structure of the wall and draw back the fortified line, owing to the attacks conducted against the city by the Romans during the First Punic War, immediately before the final conquest of Panormos, which took place in 254 BCE.

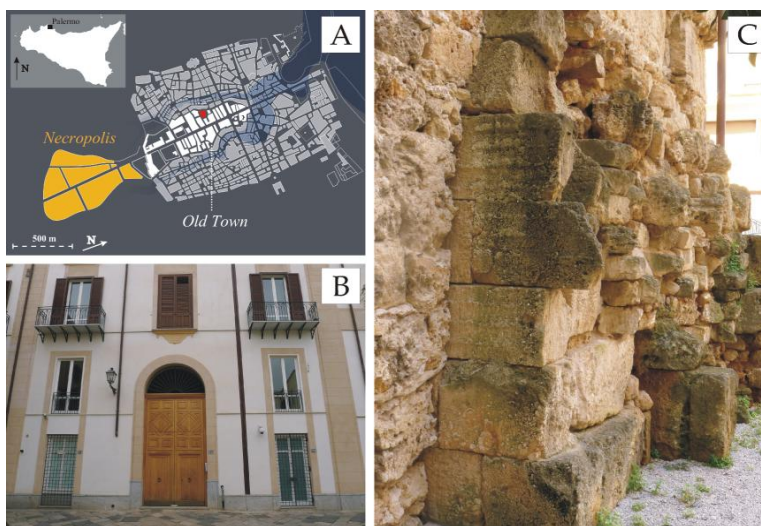


Fig. 1. Ancient Panormos: (A) A schematic map; (B) The monumental complex of the Monastero del Gran Cancelliere after recent restoration; (C) A portion of the defense wall, composed of large local biocalcarenite blocks.

Description of studied materials and analytical methods

The archaeometric investigations were carried out on a set of representative samples, made up of 11 lime-based mortars recovered from the aforementioned Roman-Punic residential environment and thus dating back to the 4th-3rd century BCE (Fig. 2A).

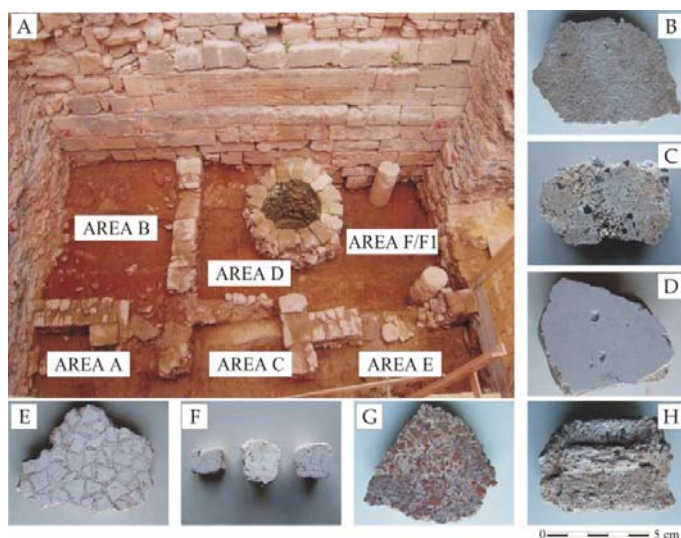


Fig. 2. Archaeological excavations area: (A) The residential environment discovered during the archaeological excavations; (B-H) The macroscopic appearance of analysed samples.

The archaeological findings in this site also included other classes of natural and artificial building materials, such as calcarenites, unfired clay bricks and a number of ceramic shards, the study of which could constitute a pertinent objective regarding the continuation of our research. The lime-based mortars subject to sampling have different utilizations, as specified in Table 1, in which a list of all the considered specimens with the indication of sampling points may be found. Most of the samples are represented by fragments of rendering mortars (7 samples, out of a total of 11) covering the partition walls of the residential environments (Figs. 2B, 2C and 2D). The rest of the samples are represented by bedding mortars used for the decoration of floors with white tesserae (samples A2, A9 and subsamples A2-T and A9-T, Figs. 2E and 2F), or with *cocciopesto* - *opus signinum* (sample A17, Fig. 2G) and by a high-relief frame with aesthetic functions (sample A1, Fig. 2H). All the wall mortars are placed on blocks made of local calcarenite. This building stone, well studied in previous works, is characterized by a secondary calcite cement, which offers a compressive strength of 10-30 mPa, as well as open porosity values ranging between 10-15% [18].

A first macroscopic description of the analysed samples was carried out according to the UNI 11176-2006 norm. The majority of them are made up of a single layer, with the exception of samples A10, A15 and A31, which are characterized by two or more layers (Table 1). Colours vary from white to pink and have been assessed by means of Munsell charts (Table 1).

Table 1. Sampling point, utilization and macroscopic description of the analysed mortars.

| Sample code | End-use | Sampling point | Number of layers | Thickness | Temper size | Colour | Bond strength |
|-------------|-------------------|---------------------------|------------------|--|---------------------------------|-------------------------------------|---------------|
| A1 | high relief frame | Area B, SU 41 | 1 | 15-20mm | medium sand | 5YR 8/1 | high |
| A2 | floor | SU 84 in SU 81 | 1 | 15mm | medium sand | 10YR 8/1 | high |
| A2-T | tesserae | SU 84 in SU 81 | 1 | up to 1cm | - | 10YR 8/1 | high |
| A4 | wall plaster | Area B, SU 41 | 1 | 15-20mm | medium sand | 5YR 8/2 | low |
| A8 | wall plaster | South side of SU 41 | 1 | 20mm | coarse sand | 2.5Y 8/3 | low |
| A9 | floor | Area F, SU 81 | 1 | 15-20mm | medium sand | 10Y 8/1 | low |
| A9-T | tesserae | Area F, SU 81 | 1 | up to 1cm | - | 10Y 8/1 | high |
| A10 | wall plaster | Area F, SU 81 | 2 | 15-20mm (internal layer) 2mm (external layer) | medium sand fine sand | 10Y 8/1 | high |
| A15 | wall plaster | Area B, SU 41 | 2 | 10-15mm (internal layer) 8mm (external layer) | very coarse sand medium sand | 5YR 8/2 | low |
| A17 | floor | Area B, SU 41 | 1 | 10-20mm | very coarse sand | 5YR 8/1 (Binder) 2.5YR 4/6 (Temper) | low |
| A20 | wall plaster | Area D, USR 91 and USR 92 | 1 | 15mm | medium sand | 7.5YR 7/2 | low |
| A23 | wall plaster | West side of USR 46 | 1 | 12mm | medium sand | 7.5YR 7/2 | low |
| A31 | wall plaster | Column of Peristyle | 2 | 8mm (internal layer) 0.5mm (external layer) | medium sand fine sand | 5YR 8/2 | low |

Key: SU - Stratigraphic Unit, USR - Stratigraphic Unit of Covering

The average grain size falls roughly within the medium sand class (0.25-0.5). Intergranular cohesion is mostly lacking, with the exception of samples A1, A2 and A10 which demonstrated a relatively higher bond strength. Lime lumps, *opus signinum* fragments and coal particles were also recognized after visual observation.

Thin-section petrography was carried out on all the samples by a Leica DC 200 polarizing microscope equipped with a digital camera. The relative abundance of sandy aggregate (expressed in percentages, in terms of area) was determined by conventional comparative tables [19].

X-ray powder diffraction (XRPD), for the identification of mineral phases was performed on bulk samples by using a Philips X'Pert diffractometer with Cu-K α radiation (operating conditions: 40 kV and 40 mA, 2°-60° 2 θ scan range, graphite monochromator, 2° 20 min⁻¹ scan rate and 2s time constant).

Regarding the SEM-EDS analysis, samples were carbon coated and mounted with silver glue on pure aluminum stubs (10mm in diameter) prior to imaging and analysis. They were preliminarily observed by secondary electrons imaging mode (SEI), so as to emphasize the microstructure and particle morphology. Consequently, corresponding specimens were embedded in epoxy resin and accurately polished with appropriate abrasive paper and diamond paste (1 and 0.1mm for finishing), in order to allow their being used for the back-scattered electrons imaging mode (BSEI) and both their quantitative and semiquantitative microchemical analyses, with a FEI Quanta 200, equipped with an energy-dispersive spectrometer with the following operating conditions: 20 KV accelerating voltage, 1.2 nA beam current, working distance equal to 10mm and counting times up to 100s. The standard ZAF correction procedures, utilized in order to achieve a matrix effect, were applied, and the concentrations of Na₂O, MgO, Al₂O₃, SiO₂, K₂O, CaO, and FeO were thus determined. A total of 10 microanalytical runs for each sample were carried out in order to acquire more representative average binder matrix compositions.

Analytical Results

Polarized light microscopy

The analysis of thin sections under the polarized light microscope (PLM) allowed for the recognition of the main mineralogical and textural features of all the studied mortar samples which were schematically resumed in Table 2. On the basis of the results deriving from microscopic investigation, the samples were clustered into four main distinguishable 'paste recipes'.

The first and largest group, inductively named Paste C, brings together six samples: A1, A2, A4, A9, A10 (internal layer), A31 (both internal and external layers). This kind of paste is characterized by a manifestly prevalent calcareous aggregate, mainly represented by bioclasts (various proportions of calcareous algae, bryozoans, echinoderms, macroforaminifera, bivalves, gastropods) as well as fragments of calcarenite and limestone. The siliciclastic components are relatively less abundant, being mainly represented by monocrystalline and polycrystalline quartz, chert and quartzarenite fragments (Fig. 3A). The aggregate/binder ratio, obtained by a visual estimation through comparative tables, varies from 1:1 to 3:1 and accordingly aggregate packing ranges from 50% to 75%. The distribution of aggregate grains is moderately homogeneous. Grain sizes range widely, from very fine sand (0.06-0.125mm) to very coarse sand (1-2mm), despite its more often being included within medium (0.25-0.5mm) and coarse (0.5-1mm) sand classes. The roundness of the monomineral granules and rock fragments which compose the aggregate generally varies from subangular to subrounded. The binder presents a micritic texture, while also demonstrating a more or less evident aggregate optical activity. Its structure is heterogeneous, or moderately homogeneous with diffused lime lumps. Macroporosity is intergranular and intragranular (within bioclasts) as well.

The second group, named Paste S, is represented by only two samples: A20 and A23. The mineralogical composition of the sand aggregate is predominantly siliciclastic, composed of mono and polycrystalline quartz, chert, fragments of radiolarite and quartzarenite, plagioclase and K-feldspar. The calcareous component, represented by bioclasts (various proportions of calcareous algae, bryozoans, echinoderms, macroforaminifera, bivalves and gastropods), biocalcarene and fragments of limestone, is mostly sporadic (Fig. 3B). The distribution of aggregate is rather homogeneous, with a prevailing grain size corresponding to medium sand (0.25-0.5mm). The aggregate packing is comparatively high (up to 75% in area) and the aggregate/binder ratio was estimated to be approximately equal to 3:1. The roundness of monomineral granules and rock fragments varies from subrounded to rounded (in the case of siliciclastic granules, due to their relatively larger size). The binder is composed of microcrystalline calcite (micrite) and shows a clear aggregate optical activity. Its structure is quite homogeneous, with sporadic or rare lime lumps. Macroporosity is mainly intergranular.

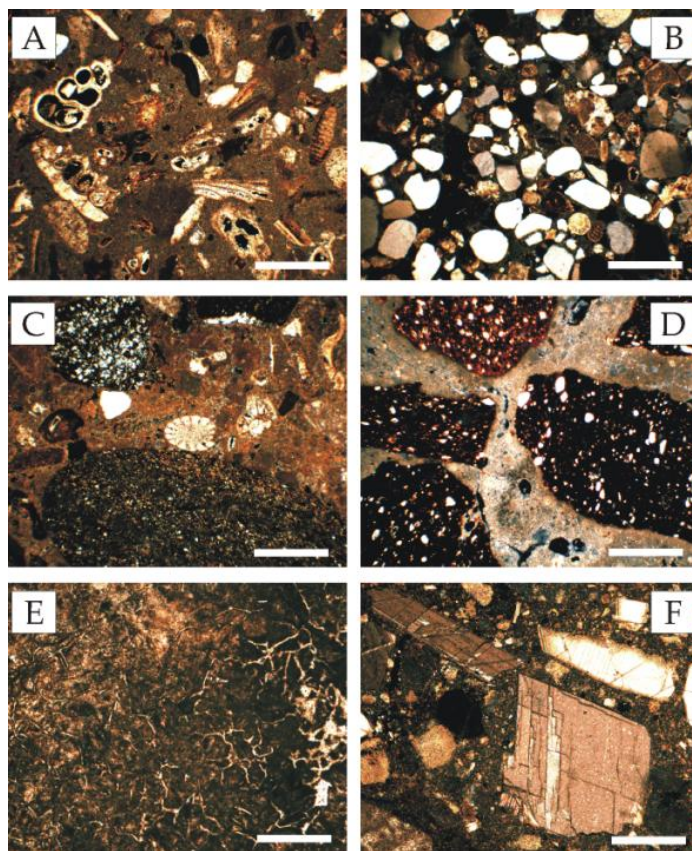


Fig. 3. Thin section microphotographs of some representative mortar' samples (crossed polars): (A) sample A1, Paste C, scale bar - 0.5mm; (B) sample A20, Paste S, scale bar - 0.5mm; (C) sample A8, Paste C/S, scale bar - 0.5mm; (D) sample A17, Paste CP, scale bar - 0.5mm; (E) microscopic features of whitish tesserae, sample A2-T, scale bar - 0.2 mm; (F) external layer of sample A10 (marmorino finishing), scale bar - 0.2mm.

The third group, here named Paste C/S, includes samples A8 and A15 (external layers). It is characterized by an aggregate consisting of approximately equivalent proportions of calcareous and siliciclastic components. Calcareous grains are mainly composed of bioclasts, limestone and calcarenite fragments (angular to sub-rounded grains). The siliciclastic components consist of quartz (both monocrystalline and polycrystalline), chert, quartzarenite

and radiolarite fragments, and, in less frequent cases, also plagioclase (Fig. 3C). Radiolarite fragments are often represented by well-rounded granules, which are attributed to the class of very coarse sand or even fine gravel. The aggregate grain distribution is rather homogeneous, with the class of coarse sand (0.5-1mm) being, generally speaking, the most abundant. The aggregate packing is highly variable, ranging from a surface area of 35% (sample A15) to 75% (sample A8), with the aggregate/binder ratio thus corresponding to 1:2 and 3:1, respectively. The binder presents a micritic texture, as well as showing aggregate optical activity. The structure is moderately homogeneous, with common lime lumps. Macroporosity is intergranular and subordinately intragranular.

Table 2. Petrographic descriptions after thin sections observation at the polarizing microscope.

| Sample code | Aggregate | | | | Binder | | | Aggregate/binder ratio | | | | |
|----------------------|----------------------|-------------|---------------|--|------------------------|---|---|------------------------|--|-----------------------------|-----------------|------------------|
| | Prevailing size (mm) | Packing (%) | Sorting | Roundness | Distribution | Mineralogical phases | Rock fragments | | Coccipesto | Texture | Porosity | Optical activity |
| A1 | 0.5-1 | 60% | well sorted | R, SR (Qtz), A-SA (rock fragments/bioclasts) | homogeneous | Qtz mono-crystalline (+) Qtz poly-crystalline (tr) | bioclasts (+++), limestones (+), chert (tr), quartzarenites (tr) | - | moderately homogeneous (sporadic lime lumps) | intergranular intragranular | active | 2:1 |
| A2 | 0.25-0.5 | 50% | poorly sorted | A-SA | moderately homogeneous | Qtz mono-crystalline (+) Glauconite (tr) | bioclasts (+++), bioclastarenites (+), limestones (+) | - | not homogeneous (common lime lumps) | intergranular intragranular | active | 1:1 |
| A2-T | - | - | - | - | - | - | - | - | not homogeneous (common lime lumps) | secondary | slightly active | - |
| A4 | 0.5-1 | 50% | poorly sorted | A-SA | not homogeneous | Qtz mono-crystalline (tr) | bioclasts (+++), limestones (++) | - | not homogeneous (common lime lumps) | intergranular intragranular | slightly active | 1:1 |
| A8 | 0.5-1 | 70-75% | poorly sorted | R, SR (Qtz), A-SA (rock fragments/bioclasts) | homogeneous | Qtz mono-crystalline (+) Qtz poly-crystalline (tr) | bioclasts (+++), limestones (+), radiolarites (+++), quartzarenites (tr) | - | moderately homogeneous (sporadic lime lumps) | intergranular intragranular | active | 3:1 |
| A9 | 0.25-0.5 | 50% | poorly sorted | A-SA | moderately homogeneous | Qtz mono-crystalline (+) | bioclasts (+++), bioclastarenites (+), limestones (+) | - | not homogeneous (common lime lumps) | intergranular intragranular | active | 1:1 |
| A9-T | - | - | - | - | - | - | - | - | not homogeneous (common lime lumps) | secondary | slightly active | - |
| A10 (internal layer) | 0.5-1 | 75% | well sorted | R, SR (Qtz), A-SA (rock fragments/bioclasts) | homogeneous | Qtz mono-crystalline (+) Qtz poly-crystalline (tr), Plg (tr) | bioclasts (+++), limestones (++), chert (+), radiolarites (+), quartzarenites (+) | - | homogeneous (rare lime lumps) | intergranular intragranular | active | 3:1 |
| A10 (external layer) | 0.2-0.5 | 45% | well sorted | A | homogeneous | spatic calcite (+++) | - | - | moderately homogeneous (sporadic lime lumps) | intergranular intragranular | active | 1:1 to 1:2 |
| A15 (internal layer) | 2-3 | 40-75% | poorly sorted | A | moderately homogeneous | Qtz mono-crystalline (tr) | bioclastarenites (+) | prevalent | moderately homogeneous (common lime lumps) | intergranular intragranular | slightly active | 1:1 to 1:3 |
| A15 (external layer) | 0.5-0.7 | 35% | well sorted | R, SR (Qtz), A-SA (rock fragments/bioclasts) | moderately homogeneous | Qtz mono-crystalline (++) Qtz poly-crystalline (++) | bioclasts (+++), limestones (+), chert (tr), quartzarenites (tr) | - | moderately homogeneous (common lime lumps) | intergranular intragranular | active | 1:2 |
| A17 | 3-4 | 50-75% | poorly sorted | A | moderately homogeneous | Qtz mono-crystalline (tr) | - | prevalent | moderately homogeneous (common lime lumps) | intergranular intragranular | slightly active | 1:1 to 3:1 |
| A20 | 0.25-0.5 | 75% | well sorted | R, SR (Qtz), A-SA (rock fragments/bioclasts) | homogeneous | Qtz mono-crystalline (+++) Qtz poly-crystalline (++) Plg (+), Kfs (+) | radiolarites (++), quartzarenites (++), chert (+), bioclasts (++), bioclastarenites (tr), limestones (tr) | - | homogeneous (rare lime lumps) | intergranular intragranular | active | 3:1 |
| A23 | 0.25-0.5 | 75% | well sorted | R, SR (Qtz), A-SA (rock fragments/bioclasts) | homogeneous | Qtz mono-crystalline | radiolarites (++), quartzarenites (++), chert (+), bioclasts (++), bioclastarenites (tr), limestones (tr) | - | homogeneous (rare lime lumps) | intergranular intragranular | active | 3:1 |
| A31 (internal layer) | 0.5-1 | 65% | well sorted | R, SR (Qtz), A-SA (rock fragments/bioclasts) | homogeneous | Qtz mono-crystalline (+) Qtz poly-crystalline (+) | bioclasts (+++), limestones (+++), quartzarenites (+) | - | moderately homogeneous (common lime lumps) | intergranular intragranular | active | 2:1 |
| A31 (external layer) | 0.1-0.2 | 30% | well sorted | SA-SR | homogeneous | Qtz mono-crystalline (tr) | limestones (+++), bioclasts (tr) | - | homogeneous (rare lime lumps) | intergranular intragranular | active | 1:2 |

Legend: A=angular, R=rounded, SA=sub-angular, SF=sub-rounded; Qtz=quartz, Plg=plagioclase, Kfs=K-feldspar; +++=prevalent, ++=abundant, +=sporadic/rare, - not detected.

The fourth group, called Paste CP, is represented by samples A15 (internal layer) and A17. The main characteristic of this paste is the prevalence of *opus signinum* within the aggregate (Fig. 3D). The fragments of *opus signinum* demonstrated both textural and mineralogical characteristics, a fact which allowed for the recognition of their local provenance [20, 21]. Quartz and biocalcarene fragments are only sporadic to rare constituents. The aggregate grains show a moderately homogeneous distribution, coupled with prevailing sizes ranging from extremely coarse sand (1-2mm) to very fine gravel (3-4mm). The binder presents a microcrystalline texture, as well as slight aggregate optical activity. It should also be noted that some limited areas at the interface between the binder and the fragments of *opus signinum* do not demonstrate any optical activity and, accordingly, may present evidence of a pozzolanic reaction, therefore resulting in the formation of amorphous calcium silicate hydrates (C-S-H). The binder's structure is, in general, moderately homogeneous, with common lime lumps. Macroporosity is mainly intergranular.

The samples coded A2 and A9 (both mortars grouped in Paste C) are the floor bedding mortars which incorporate the white tesserae, respectively coded A2-T and A9-T. The latter, once subject to the polarizing microscope, revealed itself to be composed of entirely recarbonated overfired calcium oxide. No variety of sand aggregate could therefore be observed, their microstructure being rather heterogeneous, with diffused lumps (Fig. 3E). The local use of tesserae, realized by cutting the residual blocks of the overfired limestone utilized for the production of calcium oxide has been previously attested in the manufacture of floor mosaics in Palermo, during the Middle Ages and the Baroque period [18, 22]. This therefore could be the oldest known attestation of the aforementioned practice, which has continued until the present day.

Sample A10 (external layer) is representative of Marmorino lime-based plaster. It is composed of angular fragments of calcite, derived from the mechanical crushing of white marble. The prevailing size of calcite fragments ranges from 0.2mm to 0.5mm (Fig. 3F). Aggregate packing was estimated as being approximately 45%, thus corresponding to an aggregate/binder ratio of around 1:1. The binder is composed of microcrystalline calcite (micrite) and shows a clear optical activity. Macroporosity is above all intergranular.

X-ray powder diffraction

X-ray powder diffraction (XRPD) allowed corroborating and integrating the results obtained by means of optical microscopy, with special reference to the finest components of the aggregate (< 0.04mm) and, additionally, to the microcrystalline and/or cryptocrystalline binder matrix. A semi-quantitative estimation of the abundance of the recognized mineral phases is offered within Table 3.

Considering the results of the XRPD patterns in fine detail, a first interpretative consideration can be realized, regarding the white tesserae utilized in the building of mosaics (samples A2-T and A9-T). It may be noted that the only detected crystalline phase was calcite. Therefore, given that the petrographic observations suggest both that the tesserae are constituted by overfired/recarbonated limestone, and that the peaks characteristic of magnesite or hydromagnesite went unrevealed, it is reasonable to infer that the raw material utilized in the production of quicklime has been, in the present case, a variety of limestone lacking in magnesium.

Generally speaking, calcite is the predominant mineral phase in all samples relating to Paste C, while in the samples classified within Paste S and Paste CP, quartz appears to be relatively more abundant (Fig. 4). In the remaining cases (samples belonging to Paste C/S), the two phases (calcite and quartz) are present in roughly comparable amounts. K-feldspar also being detected in small quantities in the samples belonging to Paste CP (characterized by significant amounts of *opus signinum* being found within the composition of the aggregate) and the trace in the sample demonstrating a prevalence of siliciclastic aggregate (Paste S, samples A20 and A23). On the contrary, dolomite is a common phase in samples in which the calcareous aggregate is predominant or even well-represented (Paste C and Paste C/S). It is

reasonable to assume that the presence of quartz and feldspar (K-feldspar and plagioclase) peaks existent within the XRPD patterns can be attributed to the monomineralic grains and to the siliciclastic rock fragments composing the aggregate of the studied mortars. However, other abundant or relatively common crystalline phases, such as calcite and dolomite, are constituents which can theoretically be representative of both sand aggregate (where bioclasts and calcareous rocks are abundant or common) and binder.

Table 3. Semi-quantitative mineralogical composition after XRPD analysis

| Sample code | Qtz | Cal | Kfs | Dol | Mg-calcite | Arg |
|-------------------------|------|------|-----|-----|------------|------|
| A1 | + | +++ | - | + | + | + |
| A2 | - | +++ | - | tr | tr | tr |
| A2-T | - | +++ | - | - | - | - |
| A4 | tr | +++ | - | - | - | - |
| A8 | +++ | +++ | tr | + | + | tr |
| A9 | - | +++ | - | tr | tr | tr |
| A9-T | - | +++ | - | - | - | - |
| A10 | ++ | +++ | tr | + | + | + |
| (internal layer) A10 | - | +++ | - | - | - | - |
| (external layer) A15 | +++ | ++ | + | - | - | - |
| (internal layer) A15 | ++/+ | +++ | - | + | tr | +/tr |
| (external layer) A17 | +++ | ++ | + | - | - | - |
| A20 | +++ | ++/+ | tr | tr | - | - |
| A23 | +++ | ++/+ | tr | tr | - | - |
| A31 | + | +++ | - | + | tr | + |
| (internal layer) A31 | tr | +++ | - | + | tr | tr |
| (external layer) | | | | | | |

Key: Qtz = quartz; Cal = calcite; Kfs = K-feldspar; Dol = dolomite; Mg-calcite = magnesian calcite; Arg = aragonite; +++ = abundant; ++ = common; + = subordinate; tr = trace; - = not detected.

Small amounts or traces of aragonite and magnesium-calcite were detected in several samples, namely those belonging to Pastes C and C/S, and characterized by the abundance of bioclasts within the aggregate (samples A1, A2, A8, A9, A10, A15 external layer, A31). The XRPD pattern shown in Figure 5 allows for one to appreciate a distinct shoulder on the (104) peak of calcite, which can constitute a diagnosis for the presence of magnesium calcite [23]. The occurrence of both these mineralogical phases can thus be related to the presence of gastropods and bivalve shells [24, 25].

SEM/EDS

SEM observations, by SE (secondary electron) and BSE (back-scattered electron) imaging modes, allowed for the highlighting of certain structural and textural aspects of the binder matrix, not resolvable through the level of magnification achieved with the optical microscope. Furthermore, the technique allows for one to assess the level of adhesion of the aggregate grains to the binder and, simultaneously, certain features of the porous network.

For the majority of samples placed under consideration, the binder matrix consists of sub micrometric particles, which demonstrate a good adhesion towards the aggregate granules. Numerous mesopores (with a radius ranging between 0.002 - 0.05µm, according to the IUPAC classification) and macropores (with a radius of 0.05µm or higher) characterize the binder matrix (Fig. 6A). Samples A2-T and A9-T, both representative of the tesseræ decorating the corresponding flooring mortars, are, on the contrary, characterized by the absence of any variety of aggregate granules, as well as demonstrating a remarkable degree of uniformity and compactness of the binder, which in turn results in a relatively low macroporosity (Fig. 6B).

The images of sample A4, which is representative of Paste C (calcareous), placed in a proper light show an optimal adhesion of the binder to the bioclasts, which largely compose the sand aggregate (Fig. 6C). The EDS qualitative microanalysis allowed for it to be stated that the mass of the binder consists essentially of CaCO_3 . Small amounts of different elements (Si, Al, Mg) were also discovered, likely representing the effects of a partial contamination of the mortar during the extended phase of burial (Fig. 6D). A more than acceptable adhesion of the binder to the aggregate grains has also been observed in the case of the samples belonging to Paste S (which presents a prevalence of quartz and siliciclastic aggregate) and Paste C/S (Fig. 6E). On the contrary, the analysis conducted on the samples with the aggregate consisting of *opus signinum* (Paste CP, samples A15 internal layer and A17) portrayed a relatively weaker adhesion of the binder to the fragments of crushed pottery by comparison, as well as clear evidence of biodeterioration (Figs. 6F and 6G).

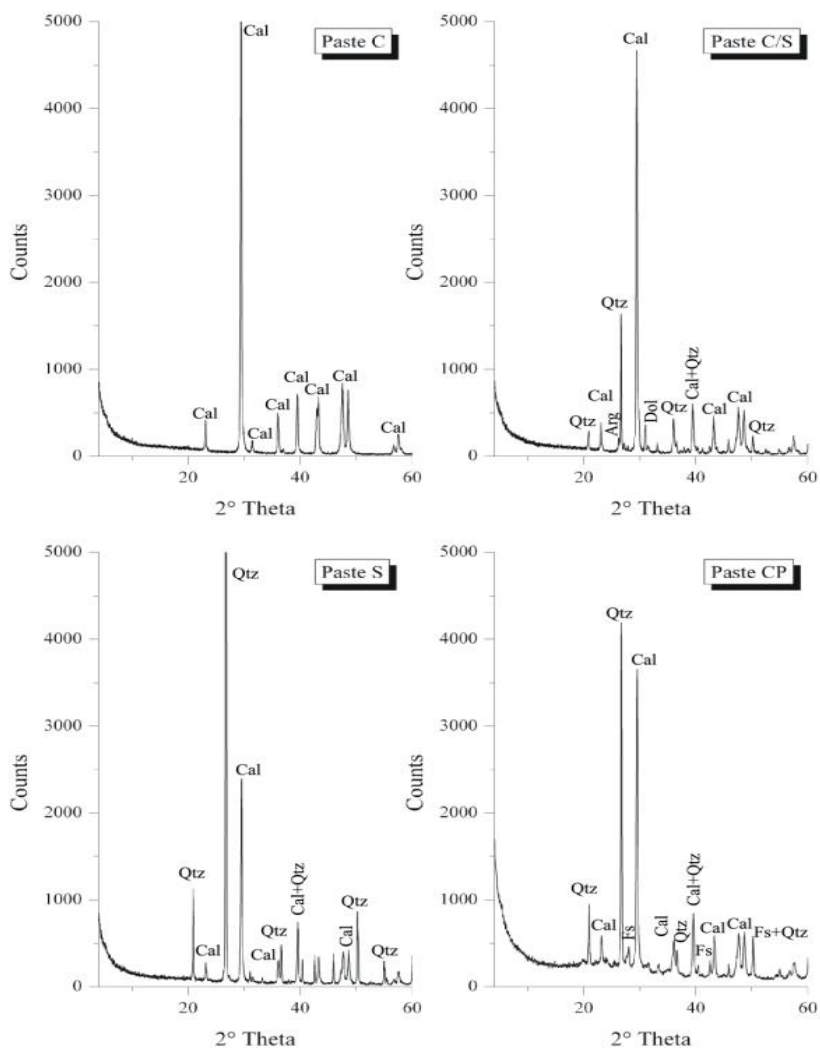


Fig. 4. XRPD diffraction patterns of representative samples of each petrographic paste. Key: Qtz - quartz; Cal - calcite; Fs - feldspars; Dol - dolomite; Arg - aragonite.

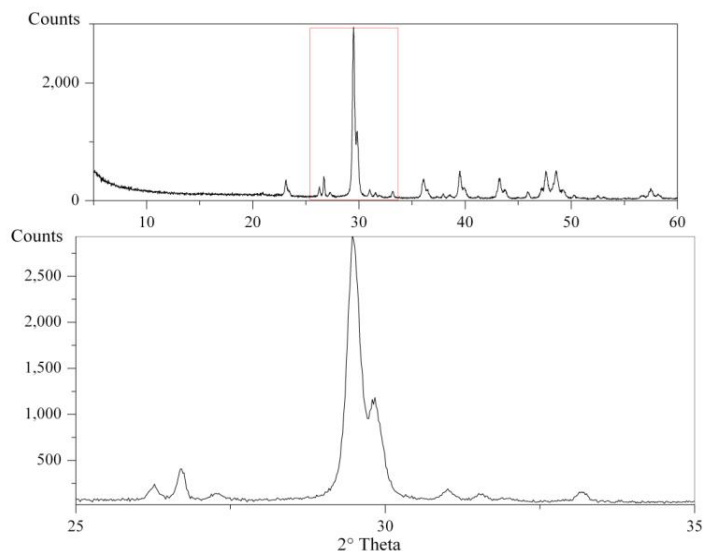


Fig. 5. The particularity of the XRPD pattern with a distinct shoulder on the (104) peak of calcite, which can be used for diagnosing the presence of magnesium calcite.

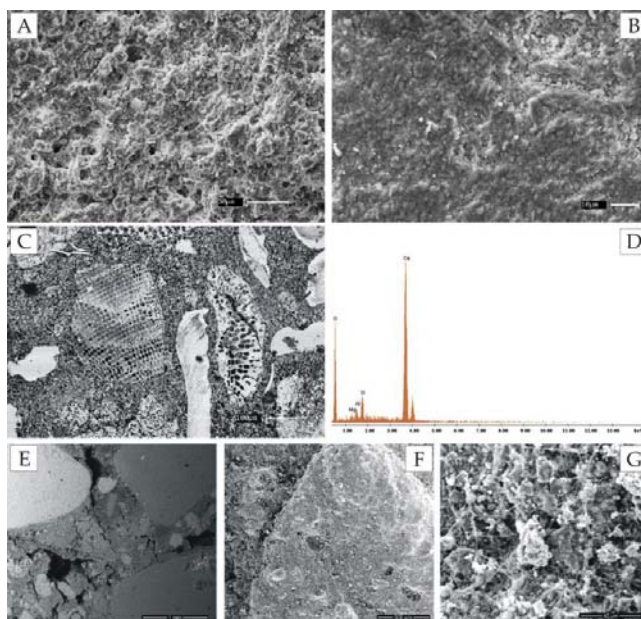


Fig. 6. SEM images of representative mortar samples: (A) SE image of binder matrix of sample A1; (B) SE image of binder matrix of sample A2-T; (C) BSE image of sample A4 portraying intergranular and intragranular porosity; (D) EDS spectrum of binder matrix of sample A4; (E) BSE image of sample A8, Paste C/S; SE images of sample A17, Paste CP, showing a relatively weaker binder adhesion to the fragments of *opus signinum* (F), as well as evidence of biodeterioration (G).

The use of quantitative EDS provided information regarding the elemental chemical composition of the binder, while also allowing for the quantification of Vicat’s ‘hydraulicity index’. Results of the micro-chemical analysis carried out upon the binder matrix (averaging values of 10 microanalytical runs for each sample) are shown in Table 5. The quantitative

analysis of the binder confirmed what was previously highlighted by XRPD-i.e. the binder is composed mainly of calcite, and can thus be classified as an aerial lime.

Table 4. Chemical analysis of the binder matrix by quantitative EDS (average values of 10 microanalytical runs for each sample).

| Sample code | Na ₂ O | MgO | Al ₂ O ₃ | SiO ₂ | P ₂ O ₅ | K ₂ O | CaO | TiO ₂ | MnO | FeO | HI |
|-------------|-------------------|------|--------------------------------|------------------|-------------------------------|------------------|-------|------------------|------|------|------|
| A1 | 0.51 | 0.94 | 1.84 | 2.16 | 0.37 | LDL | 93.30 | 0.22 | 0.40 | 0.25 | 0.05 |
| A2 | 0.58 | LDL | 2.40 | 1.14 | 0.35 | LDL | 95.00 | 0.47 | 0.06 | LDL | 0.04 |
| A4 | 0.58 | 0.26 | 1.21 | 1.84 | 0.74 | 0.18 | 93.79 | 0.52 | LDL | 0.87 | 0.04 |
| A8 | 0.99 | 0.33 | 4.87 | 1.70 | 0.36 | 0.06 | 91.23 | 0.39 | 0.09 | LDL | 0.07 |
| A9 | LDL | 0.34 | 0.40 | 2.63 | 0.80 | 0.01 | 95.82 | LDL | LDL | LDL | 0.03 |
| A10 | 0.46 | 1.15 | 2.53 | 2.38 | 1.01 | LDL | 91.76 | 0.34 | 0.33 | 0.04 | 0.05 |
| A15 | 0.85 | 0.64 | 4.14 | 1.91 | 1.19 | 0.00 | 90.46 | LDL | 0.64 | 0.17 | 0.07 |
| A17 | 0.53 | 0.63 | 5.49 | 1.80 | 0.43 | LDL | 89.59 | 0.65 | 0.43 | 0.44 | 0.09 |
| A20 | 1.36 | 0.47 | 8.19 | 4.11 | 0.47 | 0.24 | 84.57 | 0.32 | 0.27 | LDL | 0.14 |
| A23 | 0.91 | 0.55 | 7.12 | 0.97 | 0.64 | 0.14 | 89.26 | 0.15 | 0.20 | 0.06 | 0.09 |
| A31 | 0.54 | 0.66 | 2.39 | 2.23 | 1.04 | 0.04 | 92.06 | 0.22 | 0.25 | 0.58 | 0.06 |

Key: LDL - Lower than Detection Limit; HI - Hydraulicity Index

Discussion

The analyses carried out by the utilization of the PLM, XRPD and SEM-EDS technologies allowed highlighting different "recipes", utilized for the formulation of the studied mortars.

Firstly, judging by the mineralogical and chemical compositions, it was possible to establish that the binder was constantly obtained by the calcination of local carbonate rock lacking in magnesium and relatively free from other impurities (clayey residue, quartz or other substances of a similar nature). However, the classification carried out on the basis of the compositional and textural aspects of the sandy aggregate appears to be much more distinctive. To be perfectly exact, four such 'recipes' have been recognized as being essentially differentiable, on the basis of the mineralogical composition and/or relative abundance of specific components of the aggregate and, indirectly, in terms of the aggregate/binder ratio.

Generally speaking, the results obtained from the mineralogical and petrographic analyses allowed for it to be stated that, in order for the manufacture of the Hellenistic-Roman mortars subject to the present study and brought to light at Palermo to be carried out, local alluvial sands were used, most likely extracted from the coastal area adjacent to the mouth of the River Oreto (situated within the vicinity of the ancient 'Paleopolis'). This assumption is documented primarily by the numerous references found in archived documents and historical texts relating to the old building of Palermo [26, 27]. Only in the case of constructions aided by the use of crushed white marble (sample A10), flooring made up of tesserae derived from overfired calcium oxide (as confirmed by samples A2-T and A9-T) or *opus signinum* (as proven by sample A15's internal layer and also sample A17), the intentional technological choices can be clearly highlighted (such as the addition of aggregate obtained using natural or artificial raw materials) with the aim of achieving specific technical and/or aesthetic performances. Therefore, in the vast majority of cases, the composition of the aggregate fully reflects the lithotypes cropping out in the plain of Palermo and eroded by the Oreto River on its way from the spring to the mouth [28], as can be observed even by thin section observation of recent alluvial sand (Fig. 7). The different proportions between the carbonate and the siliciclastic fractions, documented after the thin-section observation at the polarizing microscope, can reasonably be interpreted as an effect caused by the choice of different supply points from time to time, otherwise as a reflection of natural variability of the alluvial deposits of the aforementioned river. In fact, none of the recipes classified with Paste C, Paste S and Paste C/S would seem explicitly functional to a specific use.

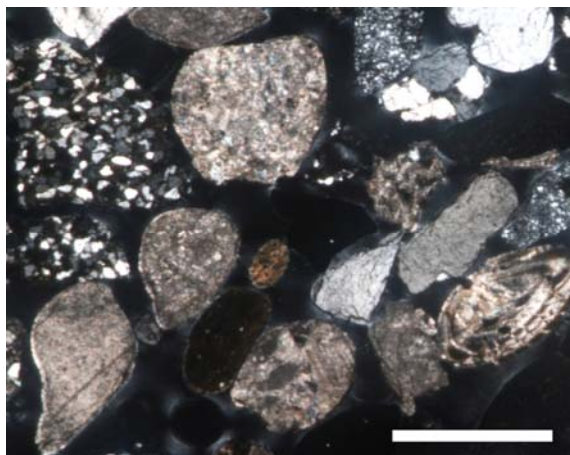


Fig. 7. Microphotograph at the polarizing microscope of the alluvial sand of the Oreto River (crossed polars, scale bar - 1 mm). Clearly recognizable bioclasts, limestones fragments, monocrystalline and polycrystalline quartz, as well as quartzarenite fragments are all clearly recognizable.

The so-called ‘battuto a cocciopesto’ (Paste CP) - the mixture of *opus signinum* - represents a paving technique frequently used in Roman times. Flooring made in this way, still well preserved after more than two thousand years, testifies to the great efficiency of a method of this nature (i.e. a mixture of aerial lime-based mortars and *opus signinum*, or, in several cases, also with the addition of pozzolanic ash). Once it has been well adjusted and smoothed out, this variety of mortar was able to ensure an excellent mechanical resistance and, at the same time, a good level of elasticity and insulation performance, as well as being aesthetically pleasing.

As unusual as agreeable to the eye, the flooring made up of white tesserae (samples A2/A2-T and A9/A9-T) was obtained in an economical manner, through the profiling of overfired limestone (waste), likely in the same furnaces that supplied the calcium oxide, with the intention of substituting a far more precious material, such as white marble.

As previously stated, Punic-Roman mortars in Palermo have never been studied from a mineralogical and petrographical perspective, while historical mortars and plasters, mostly manufactured in the Baroque and Neoclassic periods, were quite recently characterized in terms of their compositional and textural features. It is therefore interesting to compare the analysed mortars with virtually coeval materials recovered from archaeological sites in western Sicily, as well as the mortars utilized in the construction of the noble buildings of Palermo (dating back to the 17th-19th centuries AD) in order to compare the raw materials used, as well as their specific formulations.

A first comparison was made with the mortars of Hellenistic-Roman age (II-I century BCE) sampled in the Casa di Navarca at the archaeological site of Segesta (western Sicily, between Palermo and Trapani), which was a residential building with decorations of great value. These materials were analysed only by optical microscopy, more than a decade ago [29]. Although they have shown slightly different textural characteristics, as compared to the mortars subject to analysis within the present study, (i.e. containing approximately 50% of the total area and possessing an aggregate/binder ratio of 1:1), a certain similarity is found, regarding that which concerns the composition of the sandy aggregate. To be exact, they are mainly characterized by a siliciclastic component (mono and polycrystalline quartz, fragments of quartzarenites or chert), which is relatively more widespread than the carbonate equivalent (which essentially consists of calcilutite fragments, rich in planktonic foraminifera). Another similarity is the use of crushed white marble or spathic calcite as an aggregate within certain finishing layers, a fact which was also highlighted in the case of sample A10, as pertaining to the residential environment subject to the present study. In this case, however, the packing of

calcite crystals appears somewhat higher, averaging approximately 60% of the total area, whereas the binder matrix is composed in both cases of high calcium aerial limestone.

A second comparison can be made with mortars dating back to the 1st century BC, collected from the area of the Valle dei Templi and also from the medieval church of San Nicola in the city of Agrigento [30]. Also, in this case, the comparison allows one to establish similarities with the almost coeval manufactures of Palermo. The binder consists of calcium limestone (with only slight traces of magnesium), whereas the aggregate consists of mixed siliciclastic and carbonate sand, likely exploited from the alluvial deposits of the River Platani, situated a few kilometers west of Agrigento, or from bioclastic sands belonging to the Agrigento Formation (Lower Pleistocene), also outcropping in the Valle dei Templi. Both the packing and aggregate/binder ratio (with values of 60-75%, 2: 1 and 3: 1, respectively) roughly conform with Palermo' mortars. The predominant particle size distribution (0.25-2mm) and sorting (which is sparse in terms of its development) are similarly comparable.

A third comparison was made with the historical mortars of Palermo, manufactured in the post-Baroque period in order to verify the continuity of local 'material culture' and the criteria of selection of raw materials [8-11, 18]. They can be divided into three main formulations: 1) carbonate component prevails over silicoclastic; 2) carbonate and silicoclastic components are roughly equivalent; 3) silicoclastic component prevails over carbonate. It seems clear that a categorization of this nature has been found even in the mortars analysed within the present study. Even from a compositional and mineralogical perspective, the aggregate grains are represented by the same material categories, i.e. mono and polycrystalline quartz, chert, quartzarenites and radiolarites in the silicoclastic segment, and bioclasts, fragments of biocalcarenes, limestone and dolomitic limestone in carbonate components. However, important differences can be highlighted within the binder matrix, which is composed of magnesium calcite, due to the successive use of different raw materials for calcination procedures. Otherwise stated, dolomite and dolomitic limestones which are part of the Fanusi Formation and quarried from the slopes of Monte Cuccio and Monte Caputo are both located to the south of the city of Palermo [9].

Therefore, regarding the aforementioned results, it may be stated that, at a regional scale (consisting, in the present case, of western Sicily), there is a significant correlation between the coeval mortars, as concerns the manufacturing sites of Agrigento and Segesta. This correlation, which exists in terms of aggregate composition and also the relative proportion between the studied Punic-Roman mortars and the more recent historical mortars of Palermo presents a similar degree of interest. The obtained results showed that, in terms of the selection criteria of raw materials (sandy aggregate), there is a continuity dictated by the qualitative characteristics of locally available geomaterials.

Conclusions

Mineralogical and petrographic investigations have led to a complete and comprehensive characterization of the mortars from the excavation operated by the Soprintendenza BB.CC.AA. of Palermo at the Monastero del Gran Cancelliere.

The obtained results have allowed us to discover, for the first time, the "recipes" utilized within Palermo for the formulation of lime-based mortars with different functionalities, during the Hellenistic-Roman age. In particular, diversifiable formulations in relation to the quality and/or relative proportions of the sandy aggregate constituents have been highlighted. Generally speaking, the different proportions of calcareous sand (bioclasts and various lithic fragments) and siliciclastic sand (monocrystalline and polycrystalline quartz, sandstones, chert, radiolarites), mixed with an aerial binder, establish a link with the more or less contemporaneous productions of Agrigento and Segesta (which constitute an object of previous studies). Equally remarkable is the technological association existent between the relatively more modern formulations attested in the mortars' process of manufacture in the noble buildings of Palermo dating back to the 17th -19th centuries and the mortars studied in this paper.

In conclusion, these results also allowed for the deduction of the fact that, regarding the centuries-old formulation of mortars at Palermo and, additionally, the subsequent selection of the corresponding raw materials (sand for the aggregate and carbonate rocks for the production of quicklime), there is a more than satisfactory continuity. It is reasonably dictated both from the qualitative characteristics of the local geomaterials and their easy availability.

Finally, in the light of the achieved results, suitable restoration mortars manufactured with raw materials compatible with the original ones can be purposefully designed.

References

- [1] J. Elsen, *Microscopy of historic mortars – A review*, **Cement and Concrete Research**, **36**, 2006, pp. 1416–1424.
- [2] A. Moropoulou, A. Bakolas, K. Bisbikou, *Investigation of the technology of historic mortars*, **Journal of Cultural Heritage**, **1**, 2000, pp. 45–58.
- [3] A. Moropoulou, K. Polikreti, A. Bakolas, P. Michailidis, *Correlation of physicochemical and mechanical properties of historical mortars and classification by multivariate statistics*, **Cement and Concrete Research**, **33**, 2003, pp. 891–898.
- [4] F. Carò, M.P. Riccardi, M.T. Mazzilli Savini, *Characterization of plasters and mortars as a tool in archaeological studies: the case of Lardirago castle in Pavia, Northern Italy*, **Archaeometry** **50**, 2008, pp. 85–100.
- [5] S. Pavia, S. Carò, *An investigation of Roman mortar technology through the petrographic analysis of archaeological material*, **Construction and Building Materials**, **22**, 2008, pp. 1807–1811.
- [6] J. Sanjurjo-Sánchez, M.J. Trindade, R. Blanco-Rotea, R. Benavides Garcia, D. Fernández Mosquera, *Chemical and mineralogical characterization of historic mortars from the Santa Eulalia de Bóveda temple, NW Spain*, **Journal of Archaeological Science**, **37**, 2010, pp. 2346–2351.
- [7] N. Chiarelli, D. Miriello, G. Bianchi, G. Fichera, M. Giamello, I. Turbanti Memmi, *Characterisation of ancient mortars from the S. Niccolò archaeological complex in Montieri (Tuscany – Italy)*, **Construction and Building Materials**, **96**, 2015, pp. 442–460.
- [8] G. Montana, *Mineralogical-petrographic characterization of plasters by BSE images and their digital processing*. **Science and Technology for Cultural Heritage**, Vol. 4 (2), 1995, pp. 23-31.
- [9] G. Montana, *Materiali e tecnologia di produzione della calce a Palermo nei secoli passati: implicazioni nel restauro dell'architettura monumentale barocca e neoclassica*. **Mineralogica et Petrographica Acta**, **9**, 1997, pp. 373-383.
- [10] R. Alaimo, L. Di Franco, V. Gagliardo Briuccia, R. Giarrusso, G. Montana, *Plasters from the historical buildings of Palermo (Sicily): raw materials, causes and mechanisms of decay*. **Proceeding of IVth International Symposium on the Conservation of Monuments in The Mediterranean Basin**. 6th-11th May 1997, Rodi, Vol. 1, pp. 53-64. (A. Moropoulou, F. Zezza, E. Kollias, I. Papachristodoulou Eds).
- [11] R. Alaimo, R. Giarrusso, G. Montana, G. Polizzi, *Le malte da intonaco del centro storico di Palermo: materie prime, composizione e meccanismi di degrado*. **Proceeding of Congresso Nazionale della Società Italiana di Archeometria (AIAR)**, 2-3 Dicembre 1999, Verona, Vol. 1, 2000, pp. 265-276, Patron Editore, Bologna.
- [12] G. Fatta, *Intonaci a Palermo. Materiali e tecniche costruttive nella tradizione palermitana-Parte I. Recupero e Conservazione*, **24**, 1998a, pp. 26-39.
- [13] G. Fatta, *Intonaci a Palermo. Materiali e tecniche costruttive nella tradizione palermitana-Parte II. Recupero e Conservazione*, **25**, 1998b, pp. 32-44.
- [14] L. Randazzo, G. Montana, R. Alduina, P. Quatrini, E. Tsantini, B. Salemi, *Flos Tectorii degradation of mortars: An example of synergistic action between soluble salts and biodeteriogens*. **Journal of Cultural Heritage**, **16**, 2015, pp. 838–847.
- [15] C.A. Di Stefano, *Le fortificazioni*, in **Palermo Punica. Catalogo della mostra** (Palermo, 6 dicembre 1995-30 settembre 1996), Palermo 1998, pp. 85-91.

- [16] F. Spatafora, *Palermo: la città punico-romana. Guida breve*. Regione siciliana. Assessorato regionale dei beni ambientali, culturali e della pubblica istruzione. Dipartimento dei beni culturali e ambientali e dell'educazione permanente, 2005, pp. 1-56.
- [17] F. Spatafora, *Rassegna d'archeologia: scavi nel territorio di Palermo (2007-2009)*. **Atti delle Settime Giornate Internazionali di Studi sull'Area Elima e la Sicilia Occidentale nel Contesto Mediterraneo, Sicilia occidentale - Studi, rassegne, ricerche**. Edizioni della Normale, Pisa, 2012, pp. 13-22.
- [18] R. Alaimo, R. Giarrusso, G. Montana, *I materiali lapidei dell'edilizia storica di Palermo. Conoscenza per il Restauro*, Ilionbooks, Enna, 2008.
- [19] A.J. Matthew, A.J. Woods, C. Oliver, *Spots before the eyes: new comparison charts for visual percentage estimation in archaeological material*, **Recent Developments in Ceramic Petrology** (Editors: A. Middleton and I. Freestone), ISBN 086159 081 3, **British Museum Occasional Paper, 81**, 1991, pp. 211-263.
- [20] G. Montana, M.Á. Cau Ontiveros, A.M. Polito, E. Azzaro, *Characterisation of clayey raw materials for ceramic manufacture in ancient*, **Applied Clay Science, 53**(3), 2011, pp. 476-488.
- [21] G. Montana, L. Randazzo, *Le ricerche archeometriche: la caratterizzazione delle produzioni di anfore punico-siciliane*. In: Bechtold B (ed.) (2015) *Le produzioni di anfore puniche della Sicilia occidentale (VII-III/II sec. a.C.)* (con i contributi di G Montana, L Randazzo e K Schmidt), **Carthage Studies 9**, pp. 118-146.
- [22] R. Longo, R. Giarrusso, *L'impiego del palombino e del litotipo artificiale stracotto NELL'OPUS SECTILE DEL MERIDIONE NORMANNO*, **Proceedings of XVI Colloquio dell'Associazione Italiana per lo Studio e la Conservazione del Mosaico** (Editor: C. Angelelli), Palermo, 17-19 Marzo 2010. Editore Scripta Manent, Tivoli, 2010, pp. 229-242.
- [23] J. Titschack, F. Goetz-Neunhoeffler, J. Neubauer, *Magnesium quantification in calcites [(Ca,Mg)CO₃] by Rietveld-based XRD analysis: Revisiting a well-established method*. **American Mineralogist, 96**(7), 2011, pp. 1028-1038,
- [24] G. Schifano, *Temperature-magnesium relations in the shell carbonate of some modern marine gastropods*. **Chemical Geology, 35**(3-4), 1982, pp. 321-332.
- [25] G. Schifano, P. Censi, *Oxygen and carbon isotope composition, magnesium and strontium contents of calcite from a subtidal "Patella coerulea" shell*. **Chemical Geology, 58**, 1986, pp. 325-331.
- [26] A. Mazzè, **I luoghi sacri di Palermo, fonti, documenti e immagini: le parrocchie**. Flaccovio S.F. Ed., Palermo, 1979, p. 295.
- [27] D. Scinà, *La topografia di Palermo e dei suoi contorni*, **Dalla Reale Stamperia**, Palermo, 1815.
- [28] R. Catalano, G. Avellone, L. Basilone, A. Contino, M. Agate, C. Di Maggio et alii, **Carta geologica d'Italia alla scala 1:50.000 e note illustrative del Foglio 595 – Palermo**, Ed. ISPRA, Servizio Geologico d'Italia. Roma, 2013, p. 218.
- [29] D. Daniele, *Gli stucchi della villa Ellenistico - Romana di Segesta (Casa del Navarca): studio dei materiali e della tecnica di messa in opera*, **Atti delle "Terze Giornate Internazionali di Studi sull'Area Elima"**, Gibellina-Erice-Contessa Entellina 23-26 Ottobre 1997, Scuola Normale Superiore di Pisa, 2000.
- [30] G. Vella, *Le malte da intonaco degli edifici monumentali ed archeologici dell'area di Agrigento*. **Degree Thesis – Università degli Studi di Palermo**, 2004.

Received: August, 10, 2016

Accepted: September, 25, 2016